# DESIGN AND CHARACTERIZATION OF PORTABLE DMFC POWER SUPPLY SYSTEM

by

Cedric A. Jacob

A thesis submitted to the Faculty of the University of Delaware in partial fulfillment of the requirements for the degree of Bachelors of Science in Mechanical Engineering with Distinction with Distinction

Spring 2009

# DESIGN AND CHARACTERIZATION OF PORTABLE DMFC POWER SUPPLY SYSTEM

by

Cedric A. Jacob

Approved: _____

Ajay K. Prasad, PhD
Professor in charge of Senior Thesis on behalf of the Advisory Committee

Approved: _____

Suresh G. Advani, PhD
Professor in charge of Senior Thesis on behalf of the Advisory Committee

Approved: _____

Pei Chiu, PhD
Committee member from the Department of Civil Engineering

Approved: _____

Ismat Shah, PhD
Chair of the University Committee on Student and Faculty Honors

# ACKNOWLEDGMENTS

I would personally like to thank several people who were key in my ability to produce this work. First and foremost is **Srikanth Arisetty** who was a constant help and taught be how to be a good researcher. Secondly, I would like to thank **Drs. Prasad and Advani** for supporting my research and the Undergraduate Research Program for allowing this opportunity.

Several people in the research Group helped me greatly; **Doug Brunner** was excellent in helping me understand new concepts and suggesting design changes to the fuel cell to deal with problems I observed. I would also like to thank **Sudhaker Chabbra, Amir Haghilat, Feng-Yuan Zhang and Krishnan Palanichamy**.

Perhaps more than anything else, I would like to thank my family and friends — my parents and siblings who helped me by being caring and understanding; without them none of this would have been possible, and my good friends **Raymond McCauley** and **John Gangloff** for all the stimulating discussions that kept me inspired.

# TABLE OF CONTENTS

**LIST OF FIGURES** . . . . . **vi**
**LIST OF TABLES** . . . . . **viii**

**Chapter**

**1 INTRODUCTION AND BACKGROUND** . . . . . **1**

1.1 Components of a DMFC . . . . . 1

1.1.1 Polymer Electrolyte . . . . . 1
1.1.2 Gas Diffusion Layer and Catalyst Layer . . . . . 2
1.1.3 Flow Field and Bipolar Plates . . . . . 3
1.1.4 Stack Principles . . . . . 3

1.2 Benefits of DMFCs . . . . . 3
1.3 Problems with DMFCs . . . . . 4
1.4 Applications of DMFCs . . . . . 4
1.5 Past Research . . . . . 5

**2 DESIGN AND TEST METHODOLOGY** . . . . . **6**

2.1 Design Methodology . . . . . 6
2.2 Features of an Ideal Stack . . . . . 6
2.3 Testing Methodology . . . . . 7
2.4 Data Reduction . . . . . 8

**3 DESIGN: VERSION 1 FUEL CELL** . . . . . **9**

3.1 Design Parameters . . . . . 9
3.2 Test results . . . . . 10
3.3 Discussion . . . . . 10

**4 DESIGN: VERSION 2 FUEL CELL . . . . . 11**

4.1 Design Parameters . . . . . 11
4.2 Test results . . . . . 12

4.2.1 Test 1: Active Fuel, Passive Air, Active Heat . . . . . 12
4.2.2 Test 2: Active Fuel, Active Air, Active Heat . . . . . 13
4.2.3 Test 3: Passive Fuel, Passive Air, Active Heat . . . . . 14

4.3 Discussion and Diagnosis . . . . . 14

**5 DESIGN: SECOND ITERATION VERSION 2 FUEL CELL . . . 16**

5.1 Design Parameters . . . . . 16
5.2 Test Results . . . . . 16

5.2.1 Test 1: Passive Fuel, Passive Air, Active Heat . . . . . 16
5.2.2 Test 2: Passive Fuel, Passive Air, Active Heat . . . . . 18
5.2.3 Test 3: Active Fuel, Passive Air, Active Heat . . . . . 18
5.2.4 Test 4: Active Fuel (pre-heated), Passive Air, Active Heat . . 18
5.2.5 Individual Cell Testing . . . . . 18

5.3 Discussion and Diagnosis . . . . . 20

5.3.1 New MEA's . . . . . 22

**6 DESIGN: THIRD ITERATION VERSION 2 FUEL CELL . . . . 24**

6.1 Standard Testing . . . . . 24
6.2 Electrochemical Impedance Spectroscopy . . . . . 27

**7 TRANSPARENT CELL . . . . . 30**
**8 CONCLUSIONS AND FUTURE WORK . . . . . 33**

**REFERENCES . . . . . 35**

# LIST OF FIGURES


**1.1** Exploded Direct Methanol Fuel Cell . . . . . 2

**4.1** Fuel Cell Version 2+ . . . . . 12

**4.2** Polarization Curve — $4ml/min$ and $1.5M$ . . . . . 13

**4.3** Power Curve — $4ml/min$ and $1.5M$ . . . . . 14

**5.1** Polarization Curve — Room Temp, Passive Air, 1M Passive Methanol . . . . . 17

**5.2** Power Curve — Room Temp, Passive Air, 1M Passive Methanol . . 17

**5.3** Polarization Curve — Individual Cells, 2M heated methanol, $3ml/min$ . . . . . 19

**5.4** Power Curve — Individual Cells, 2M heated methanol, $3ml/min$ . 20

**5.5** Voltage with different Concentrations — New MEA's, $60°C$ . . . . 22

**5.6** Power with different Concentrations — New MEA's, $60°C$ . . . . . 23

**5.7** Impedance Spectroscopy at 4M . . . . . 23

**6.1** Polarization Curve, Passive 4M at $60°C$, Varying Air Speed . . . . 25

**6.2** Polarization Curve, Passive 6M at $60°C$, Varying Air Speed . . . . 25

**6.3** Power Curve, Passive 4M at $60°C$, Varying Air Speed . . . . . 26

**6.4** Power Curve, Passive 6M at $60°C$, Varying Air Speed . . . . . 26

**6.5** OCV — Impedence Spectroscopy . . . . . 28

**6.6** 0.45V — Impedence Spectroscopy . . . . . 28

**6.7** 0.3V — Impedence Spectroscopy . . . . . 29

**7.1** Polarization Curve . . . . . 31

**7.2** Power Curve . . . . . 31

**7.3** Images . . . . . 32

# LIST OF TABLES

**2.1** Ideal Stack Features . . . . . 7

**3.1** V1 FC vs. Ideal Stack — Characteristics . . . . . 10

**4.1** V2 FC, V1 FC, Ideal Stack — Features . . . . . 12

# ABSTRACT

The goal of this thesis is to provide an understanding of a practical portable direct methanol fuel cell (DMFC) stack system as well as produce a fuel cell stack that can be used for testing and demonstration purposes.

DMFCs are relevant because of the high energy density that the fuel (methanol) affords. However, there are several key limitations — DMFCs suffer from greater activation, ohmic, and crossover losses than a standard Hydrogen Fuel Cell, as well as having a larger restriction on maximum current draw. This combination of advantages and disadvantages makes DMFCs very practical for the portable electronics industry.

An attempt has been made therefore, to design and fabricate a DMFC *stack* that can be used in the Laboratory for testing purposes as well as attempt some innovative design modification with the hope of making either performance or size gains while keeping the stack practical and usable.

# Chapter 1

# INTRODUCTION AND BACKGROUND

Direct Methanol Fuel Cells (DMFCs) work on the oxidation reaction of methanol in order to push electrons through a circuit. The chemical equation followed is:

$$CH_3OH + 1.5O_2 \rightarrow 2H_2O + CO_2 \tag{1.1}$$

For every molecule of methanol, 6 electrons are exchanged — generating electricity. There are several technologies that help to make this possible, but fundamentally it is done through a surface reaction that allows the fuel to oxidize while conducting protons through an electrolyte and electrons through an electrode.

## 1.1 Components of a DMFC

There are several components to a fuel cell: a Polymer Electrolyte (PEM), Gas Diffusion Layer (GDL), Catalyst Layer (CL), Bipolar Plates, and Flow Feild. See Figure 1.1 for illustration.

### 1.1.1 Polymer Electrolyte

Both sides (cathode and anode) are separated by a polymer electrolyte. The electrolyte is a *proton conductor* that allows the methanol on the anode side to react with the oxygen on the cathode side but does not allow the electrons to pass (thus forcing them around the circuit.)

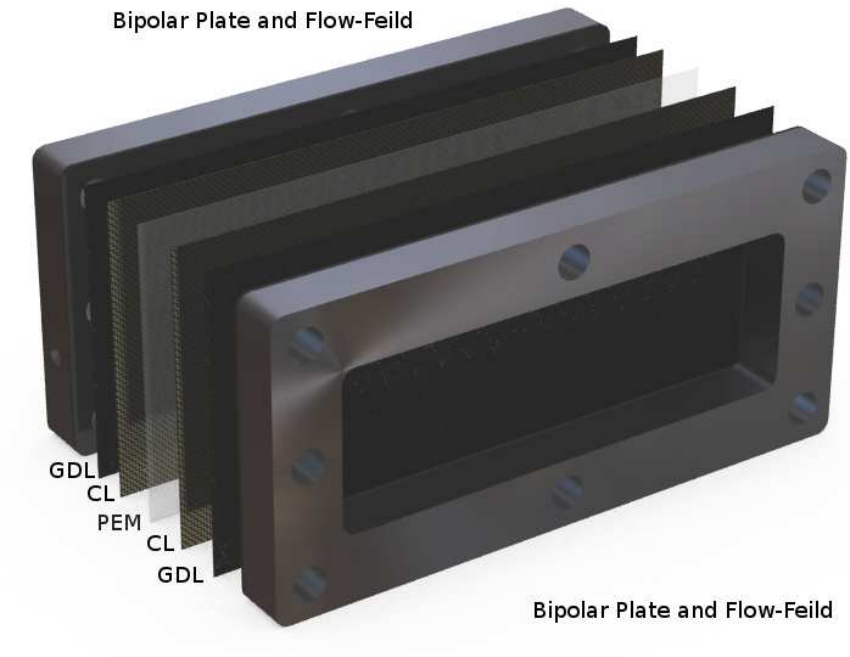


**Figure 1.1:** Exploded Direct Methanol Fuel Cell

In fuel cells within the scope of this thesis, the polymer electrolyte used is Nafion-117 manufactured by DuPont.

### 1.1.2 Gas Diffusion Layer and Catalyst Layer

The "gas diffusion layer's" purpose is to transport the oxidant and fuel towards the membrane, while the "catalyst layer" is a support structure containing nanoparticles of a catalyst material (generally Pt or Pt-Ru).

In all fuel cells within the scope of this thesis, the gas diffusion layer is a sheet of carbon cloth, and the catalyst layer is a layer of carbon black infused with Pt or Pt-Ru nanoparticles as the catalyst. Further, the catalyst layer is infused with a very thin layer of Nafion which provides a triple phase contact between the nanoparticles, carbon support, and nafion, allowing proton, electron, and molecule transport to occur — thus, the layer effectively becomes an electrode as well.

These components put together (polymer electrolyte, gas diffusion layer and catalyst layer) are collectively called an MEA (membrane electrode assembly).

### 1.1.3 Flow Field and Bipolar Plates

The next problem is how to move the fuel *to* the MEA without blocking the electron conducting paths. In order to do this there needs to be a *flow field*. Most laboratory fuel cells use either graphite or stainless steel plates with grooves machined into them in order to push a reactant flow through. The MEA then is in contact with regions where there are grooves (for fuel transport) and regions that are touching the metal of the plate (for electron conduction). Bipolar plates are used for current collection and allow the fuel cells to be put into a stack.

In all fuel cells within the scope of this thesis, a novel technique using metal foam as both the flow field *and* bipolar pate was used. The fuel can pass evenly throughout the entire foam and the electrons can pass through the metal structure. This technique allows the cells to be made smaller and with more structural rigidity. It also allows them to be stacked in a different way than has been done before — through electrode sharing. This means that two cells can share the same anode or cathode (of course it means the cell must be in parallel, see 1.1.4).

### 1.1.4 Stack Principles

"Stacking" fuel cells means to add them together either in series or in parallel electrically. When added together in parallel they increase the reaction area of the cell (which is proportional to current outputted by the cell) and when the are added together in series their voltages are added linearly.

## 1.2 Benefits of DMFCs

The main advantage of DMFCs compared to other types of fuel cells is the large energy density of methanol. Because it is a liquid and it can react directly in

an electrolytic reaction and the amount of *hydrogen* atoms per volume (and thus electrons) is much larger. This means that it is easier to transport and it occupies less space.

Methanol is also inexpensive, and is used in solutions of lower concentrations $(1 - 6M)$. This makes it even cheaper, as well and maybe more importantly means that it will not burn easily (as opposed to pure hydrogen which burns very easily in air.)

### 1.3 Problems with DMFCs

The main problem with DMFC's is methanol crossover. Methanol crossover occurs when whole methanol molecules diffuse across the electrolyte membrane without reacting (the molecules can then react on the other side.) This wastes fuel and reduces voltage by creating a mixed potential cell. DMFCs also have a lower maximum current draw (and thus power draw) and so can only be used practically for low power applications.

### 1.4 Applications of DMFCs

The main arena for DMFCs in industry is the market for portable electronics — they use enough power to justify using a fuel cell but not enough to necessitate using hydrogen. While hydrogen would be usable, it would have to be compressed, stored, and transported; also, being combustible it would also be more dangerous than a dilute methanol solution. The market is available for small scale portable electronics such as cell phones, PDA's, MP3 players and various forms of instrumentations, as well as larger scale electronics such as Laptops and Power Tools. DMFC's are also used to replace portable power generators (generally under a few hundred watts).

## 1.5 Past Research

Past research done involves testing single cells with metal foams used as a flow field (Arisetty, Jacob et al. 2008) as well as research into the optimization of DMFCs for finding the best input methanol concentration for each particular current draw. This research would ideally be applied to a full fuel cell stack and balance of plant; however, this realization requires first developing the stack.

# Chapter 2

# DESIGN AND TEST METHODOLOGY

## 2.1 Design Methodology

The design, testing, and characterization of the fuel-cell system follows a four phase design process. Phase 1 is used to define the problem and describe it in terms of what needs to be accomplished; Phase 2 is the concept generation and selection phase; Phase 3 is the design phase, and Phase 4 is the production and testing phase. After phase 4 it is important to re-iterate between phases 3 and 4 until the desired product provides the appropriate design characteristics.

## 2.2 Features of an Ideal Stack

There are several features that an ideal stack must have. These are things that it *should* have to be operational in a real-world applications oriented environment as listed in(Table 2.1).

These properties are fairly straightforward; A fuel cell must have several subsystems in order to work in a practical environment: water management, $CO_2$ management, and power management. On top of these balance of plant systems it must have a simple system for refueling and optimally be able to operate in any orientation.

Table 2.1 will be repeated and expanded throughout the thesis in order to compare the ideal stack with the ones used in the laboratory environment during testing.

**Table 2.1:** Ideal Stack Features

| Characteristic |
|---|
| $CO_2$ Removal |
| Heating System |
| Power Regulation |
| Voltage Regulation |
| Fuel Cartridges |
| Orientable |
| Water Recirculation |

## 2.3 Testing Methodology

One of the most useful sets of data that can be gathered from a fuel cell is the *polarization* curve. The curve relates voltage output to current draw and provides great insight into what type of loss mechanisms are occurring. A polarization curve then, can be used to *characterize* a fuel cell system. There are several important variables to consider when characterizing a fuel cell: cell temperature ($T$), flow rate ($Q$), voltage ($V$), current density ($mA \times cm^{-}2$), ambient temperature ($T_0$) and current run time ($s$). The stack performance is also affected by the membrane, catalyst, and gas diffusion layer.

The testing equipment used is an Arbin ©test stand (used to apply load and measure current density and voltage). Before pump integration, the fuel cell is attached to a variable flow rate methanol pump. Thermocouples and a temperature controller are used to regulate and measure temperature in the fuel cell.

The parameters that were varied during the test were:

- Temperature
- Air Flow Rate
- Methanol Flow Rate
- Load

Setting the first three parameters to zero makes that portion of the system *passive* — That means that it does not induce any parasitic power loss. Setting the last item (load) to zero gives a measurement of open circuit voltage (OCV). The temperature, air flow rate, and methanol flow rate are fixed at the beginning of the test and the voltage is measured with incremental changes of load (current density).

## 2.4 Data Reduction

The data recorded is reduced to produce a polarization curve. The steady state voltage for each specific load is tabulated with error accounted for and plotted as voltage vs. current density.

# Chapter 3

# DESIGN: VERSION 1 FUEL CELL

The first fuel cell design was done with the intention of providing an analysis on the suitability of completely passive systems towards power generation at room temperature and allow for characterization of a single cell.

## 3.1 Design Parameters

The fuel cell was designed as a single cell passive system. Air and methanol transport were designed to rely on natural convection to supply the MEA (membrane electrode assembly) with fresh fuel. Heating was designed to be passive — no heaters — relying on exothermic chemical energy to provide heat. Rather than using a bipolar plate and flow fields, a metal foam was used to improve structural properties and improve $CO_2$ bubble transport.

The MEA used had $4mg/cm^2 Pt-Ru$ on the anode side, $2mg/cm^2 Pt$ on the cathode side, a Nafion-117 membrane and an area of $10cm^2$. The current collectors were attached to the foam and the fuel storage mechanism was built out of polycarbonate and sealed with silicone. Plastic cap screws were used in order to avoid shorting out the bipolar plates.

The system characteristics can be compared to an ideal stack by using the characteristics listed in table 2.1. In table 3.1 a comparison has been drawn between this system and an ideal one.

**Table 3.1:** V1 FC vs. Ideal Stack — Characteristics

| Ideal Characteristic | FCV1 |
|---|---|
| $CO_2$ Removal | Yes |
| Heating System | No |
| Power Regulation | No |
| Voltage Regulation | No |
| Fuel Cartridges | No |
| Orientable | No |
| Water Recirculation | No |

### 3.2 Test results

The OCV produced by the cell was good at $.6V$, however when load was applied to the cell the voltage was reduced severely and the current output was insignificantly small.

### 3.3 Discussion

The poor performance with any size load is generally characteristic of large activation losses — activation losses are caused by poor reaction kinetics.

# Chapter 4

# DESIGN: VERSION 2 FUEL CELL

The second fuel cell designed was done with the intention of providing an analysis on the suitability of partially passive, partially active system. It was also designed to be stackable — that is, more than one cell could be used.

## 4.1 Design Parameters

As a variably active system, the cell was designed to be able to switch between active and passive air transport, methanol transport, and heating. Similar to the previous design, a metal foam was used for all three flow fields. The cells were stacked in parallel — this way one anode could be shared, saving space and making the cell more compact. Each block was machined out of aluminum and assembled together using machine screws surrounded by plastic tubing (to insulate the cell electrically). The methanol connections were made using luer-lock so that they could remain small and easy to use, the air ducts were holes cut into the side to allow the air to flow through passively — or through the use of a small fan if needed. Two strip heaters were placed on each side and insulated to allow heat to flow into the cell laterally. Electrical connections were made by tapping a hole on each electrode and screwing in terminals. The MEA used, as before, had $4mg/cm^2 Pt - Ru$ on the anode side, $2mg/cm^2 Pt$ on the cathode side and a Nafion-117 membrane. It measured $30cm^2$ for each cell, resulting in a net effective area of $60cm^2$. A picture of the completed fuel cell is shown in in Figure 4.1.

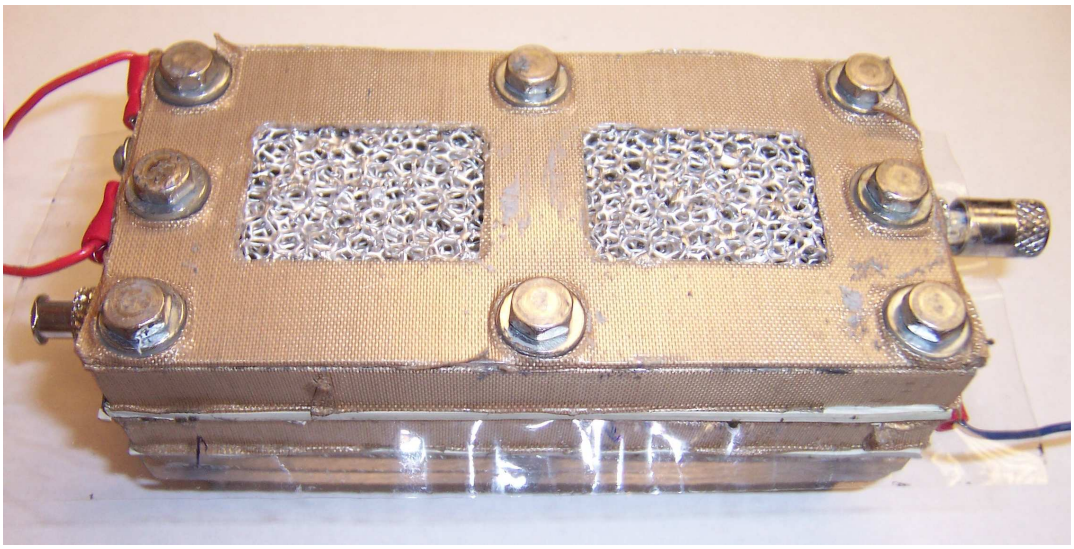

**Figure 4.1:** Fuel Cell Version 2+

**Table 4.1:** V2 FC, V1 FC, Ideal Stack — Features

| Ideal Characteristic | FCV1 | FCV2 |
|---|---|---|
| $CO_2$ Removal | Yes | Yes |
| Heating System | No | Yes |
| Power Regulation | No | No |
| Voltage Regulation | No | No |
| Fuel Cartridges | No | Partial |
| Orientable | No | No |
| Water Recirculation | No | No |

The system characteristics can be compared to an ideal stack again by using the characteristics listed in table 2.1. In table 4.1 a comparison has been drawn between this system, its predecessor and an ideal stack.

## 4.2 Test results

### 4.2.1 Test 1: Active Fuel, Passive Air, Active Heat

The first test done used a flow rate of $4ml/min$, a fuel concentration of $1.5M$ and a temperature of $50°C$. The initial results showed quite poor performance; the

OCV was $0.27V$ (see figures 4.2 and 4.3).

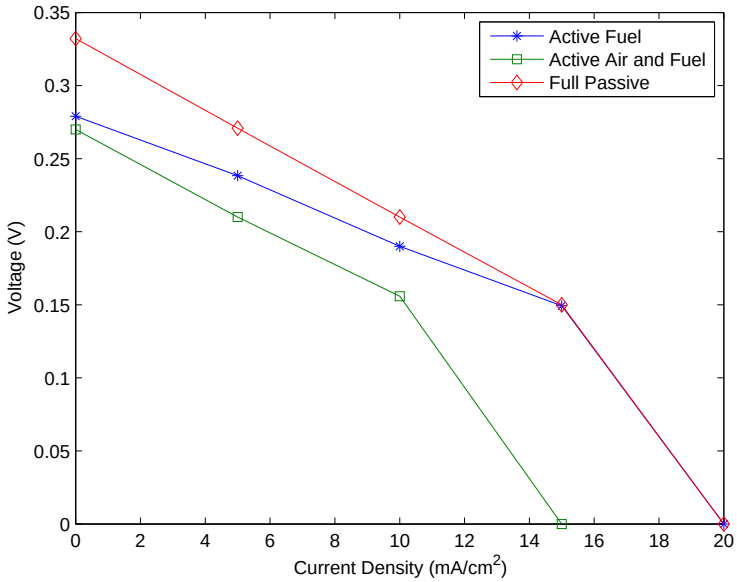


**Figure 4.2:** Polarization Curve — $4ml/min$ and $1.5M$

As the load is increased the voltage reduces linearly as can be seen on the characterization curve (see figure 4.2). The characterization curve also shows how low of a current density it takes in order to bring the cell to a dangerous voltage (dangerous in that the catalyst can become oxidized and perform poorly in the future).

### 4.2.2 Test 2: Active Fuel, Active Air, Active Heat

The second test done used a flow rate of $4ml/min$, a fuel concentration of $1.5M$, Temperature of $50°C$, and air produced by two fans on either side of the fuel cell (no quantitative data for air flow rate was recorded).

It is interesting to note that making the air active in this case actually degraded performance. The voltage was lower than the previous test in all cases. The polarization curve shows similar trends to the first and second experiment — again with lower voltages at each current density.

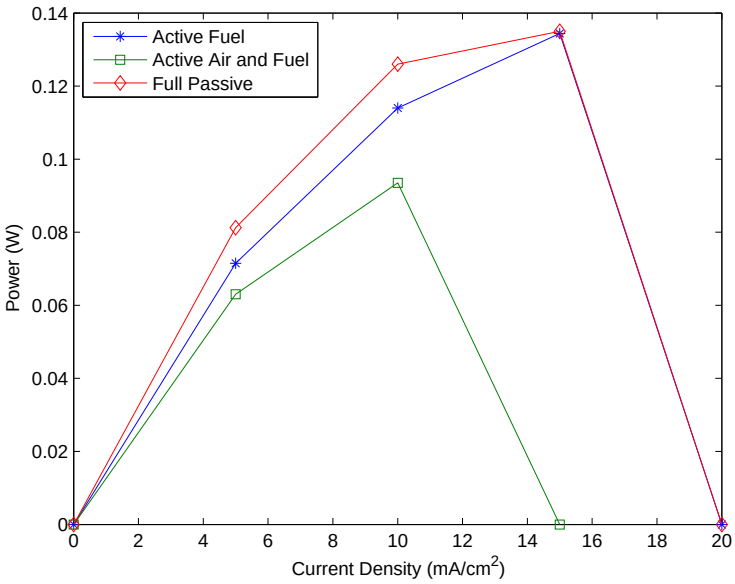


**Figure 4.3:** Power Curve — $4ml/min$ and $1.5M$

### 4.2.3 Test 3: Passive Fuel, Passive Air, Active Heat

The third test was done with only the heaters in operation. Both air and fuel were supplied passively (the cell was filled with methanol and then closed); the advantage here is better conservation of heat energy keeping the cell warmer.

## 4.3 Discussion and Diagnosis

All three tests reported poor results in the form of low OCV and highly linear losses (the voltage curve can be fitted to a line in this area.) Coupled, these two forms of losses are characteristic of an abnormally large amount of internal current. Effectively, this means that measured OCV is *actually* the cell voltage at the current density that equates to the internal current — like shifting the entire curve to the left (ideal voltage is to the left of the y-axis). The losses in this way overpower the mass transport losses, which would be at a low enough voltage that the cell would be in danger of catalyst poisoning.

Another problem noticed was the tendency of the fuel cell to dry itself out quickly when unattended and unloaded — this seemed to indicate a short circuit. In order to find the cause of such large internal currents, the stack was tested with an ohm-meter from cathode to cathode, and from anode to each cathode. Recorded values were on the order of $1\Omega$ with an open circuit and no fuel, confirming that there was an electrical short through the MEA.

In order to diagnose the problem, the stack was taken apart and resistances measured across each MEA. Reported resistances were very low (approximately $0.5\Omega$. Upon further inspection it was seen that the carbon paper was wrapping around the edges of the MEA and touching the other side — this would cause enough internal current to explain the results obtained.

# Chapter 5

# DESIGN: SECOND ITERATION VERSION 2 FUEL CELL

## 5.1 Design Parameters

In order to fix the MEA's they were taken out and the GDL was cleaned off the the membrane edges — leaving only the Nafion-117 exposed. This ensures that there are no conducting paths around the membrane. Before the process (removal of the GLD from the membrane edges) the resistance from anode GDL to cathode GDL was approximately $0.1\Omega$ (dry) and after the process it measured approximately $45\Omega$ (dry). The cell was reassembled in the same way as FCV2 and fiberglass insulation was added to either side of the heaters. Another modification added was the possibility of heating the incoming fuel before it entered the fuel cell.

The initial test on the stack (with a standard multimeter) revealed an OCV of $0.510V$ at Room Temperature, Passive Air, Passive $1M$ Methanol and no heat. Taking this as an indication of success on the part of reducing internal current the stack was characterized under several different operating conditions with the results summarized in figures 5.1 and 5.2.

## 5.2 Test Results

### 5.2.1 Test 1: Passive Fuel, Passive Air, Active Heat

The first test was set up to be passive on the fuel side, with a molarity of $2M$, heated to $50°C$ internally with passive air flow and no fuel pre-heating.

The OCV for this test was $.510V$, $1.77A$ was able to be drawn out of the cell and the maximum power obtained is just under 0.25 watt.

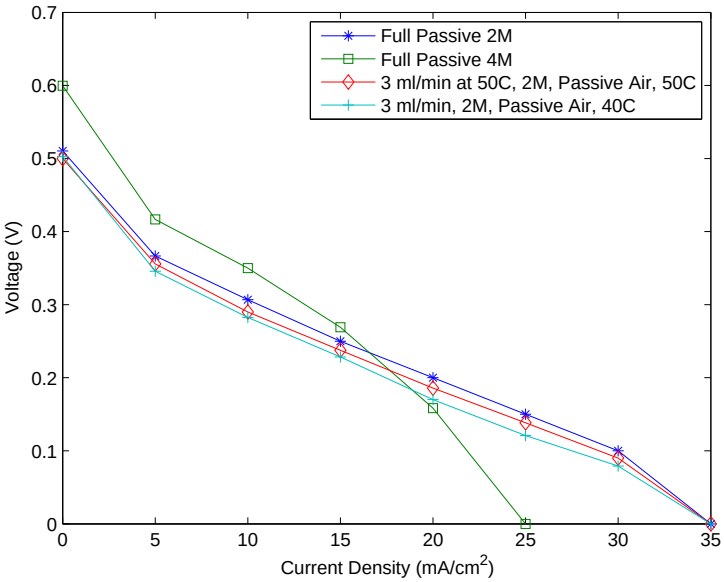


**Figure 5.1:** Polarization Curve — Room Temp, Passive Air, 1M Passive Methanol

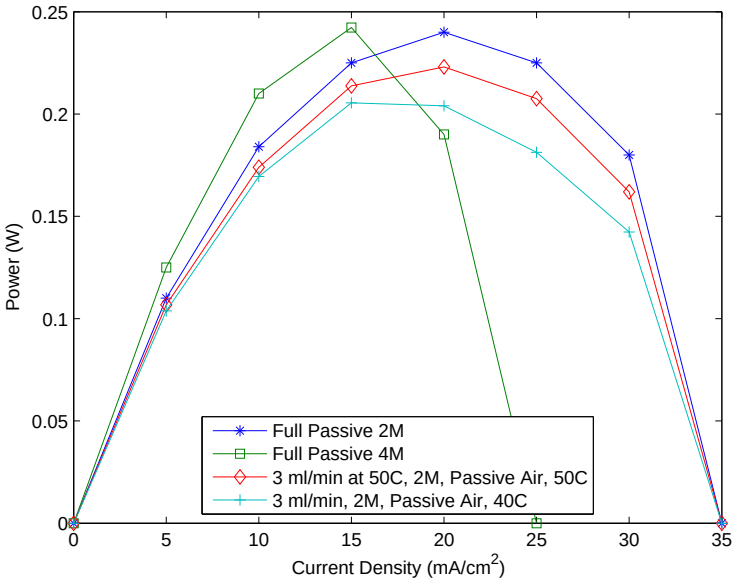


**Figure 5.2:** Power Curve — Room Temp, Passive Air, 1M Passive Methanol

### 5.2.2 Test 2: Passive Fuel, Passive Air, Active Heat

The second test was set up similarly, however the molarity of the fuel was changed from $2M$ to $4M$. Again, the methanol was not pre-heated, both sides were passive, and the stack was heated to $50°C$.

The OCV for this test started at $.69V$ and then shrunk to $.57V$ as it reached steady state conditions. It was possible to draw $1.5A$ out of the cell and the maximum power obtained is just under a 0.25 watts.

### 5.2.3 Test 3: Active Fuel, Passive Air, Active Heat

The third test was set up with an active methanol flow at $3ml/min$ and a molarity of $2M$ while the air remained passive. The methanol was *not* pre-heated but the cell was heated to $50°C$.

The OCV for this test was $.510V$, $2.1A$ was drawn from the cell and the maximum power obtained was approximately $0.2W$.

### 5.2.4 Test 4: Active Fuel (pre-heated), Passive Air, Active Heat

The fourth test was set up with an active methanol flow at $3ml/min$ and a molarity of $2M$ while the air remained passive. The Methanol was pre-heated to $55°C$ and the cell was heated to $50°C$.

The OCV for this test was $.5V$, $2.1A$ was able to be drawn out of the cell and the maximum power obtained was approximately $0.2W$.

### 5.2.5 Individual Cell Testing

In order to find out whether or not there are any differences between each cell in the stack, they were tested separately to see if the results of one cell were close to that of the other. These tests allow us to see the relative quality of each MEA and determine whether possible performance gains could be made by reducing this

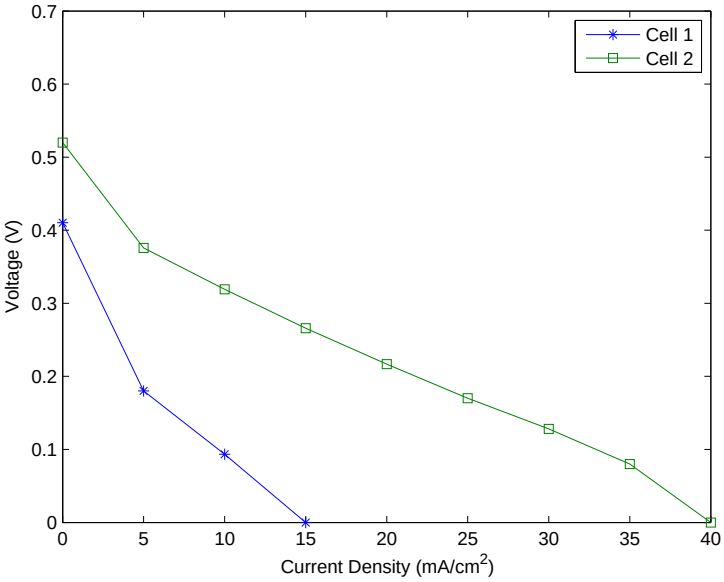


**Figure 5.3:** Polarization Curve — Individual Cells, 2M heated methanol, $3ml/min$

difference. First comparison can be made between the polarization curves of each cell as seen on figure 5.3.

The cells were tested with 2M heated methanol flow with a rate of 3 ml/min and a temperature of $50°C$. The cell was heated to $50°C$ and the air supply was passive.

Cell # 2 has a *much* higher OCV ($0.52V$ vs. $0.41V$) and much higher current output ($2.4A$ vs. $0.9A$). This shows plainly that cell # 1 is vastly under-performing Cell # 2. Since the cells are in parallel the current output should be doubled when they are put together, instead, the current is additive between the two ($3.3A$ rather than $4.8A$). The voltage is also a composite of the two, however the relationship is not linear.

It is also possible to compare the characterization and power curves of each individual cell. (see figure 5.4) These plots show a very dramatic degree of under-performance of one of the cells.

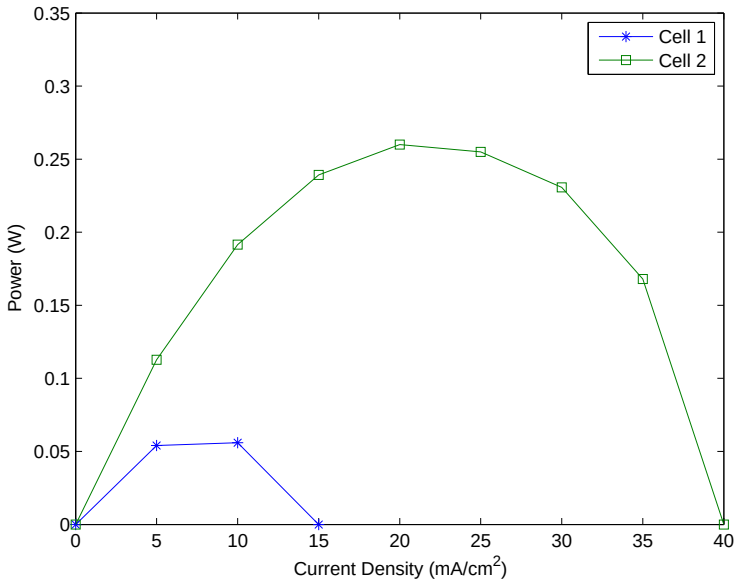


**Figure 5.4:** Power Curve — Individual Cells, 2M heated methanol, $3ml/min$

### 5.3 Discussion and Diagnosis

Figures 5.1 and 5.2 both show that all 2M tests have very similar characteristics. It can be seen that using a heated active fuel feed decreases performance, and that a non-heated active fuel feed further decreases performance. The two passive tests (2M and 4M) have similar characteristics as well, each supplying a relatively high power. The 4M test produces a slightly higher power, has a slightly higher OCV, but suffers more from losses at higher current densities. This could be a combination of mass transport losses coupled with crossover.

Another very significant result of this data are the differences between the single cell tests. Cell # 2 by itself produced more power than any other test run. This suggests that there is a loss occurring because of the poor quality of cell # 1 and furthermore implies that significant enhancement can be made by using a better MEA for cell #1. It is also important to note that since both cells have the same history, it may be possible that they are both of lower than standard quality and

that significant performance gains could be made by using better, fresher MEAs.

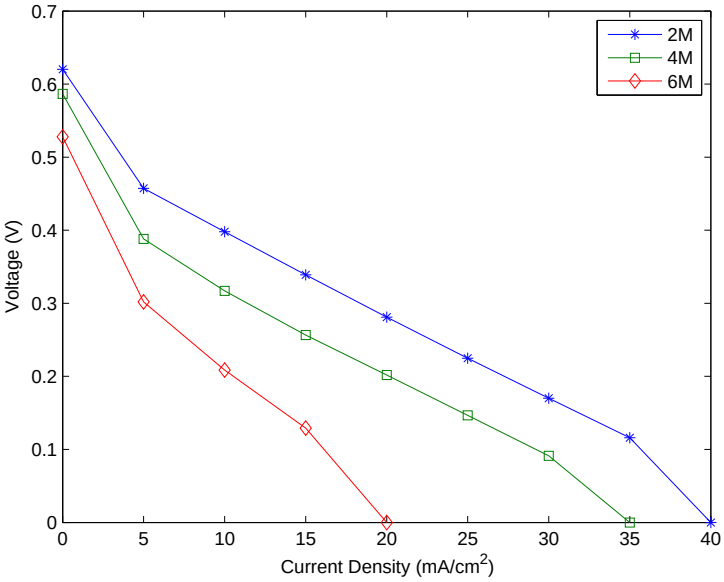


**Figure 5.5:** Voltage with different Concentrations — New MEA's, $60°C$

### 5.3.1 New MEA's

In order to test the quality of the MEA, new MEA's were inserted and the cell was retested with the same conditions (see figures 5.5 and 5.6).

Next, electrochemical impedance spectroscopy (EIS) was performed to determine how different loss mechanics affected the cell. The test was run at OCV, 0.45V, and 0.3V. The results (see figure 5.7) show a very high amount of ohmic losses. These are found by looking at the real part of the impedance when the imaginary part is zero. In all three cases (they should be identical) the impedance was rated at 0.18Ω. The EIS also shows that the cell is heavily affected by mass transport losses — this can be seen by the radius of curvature of the line that the impedance vector traces out as frequency is increased.

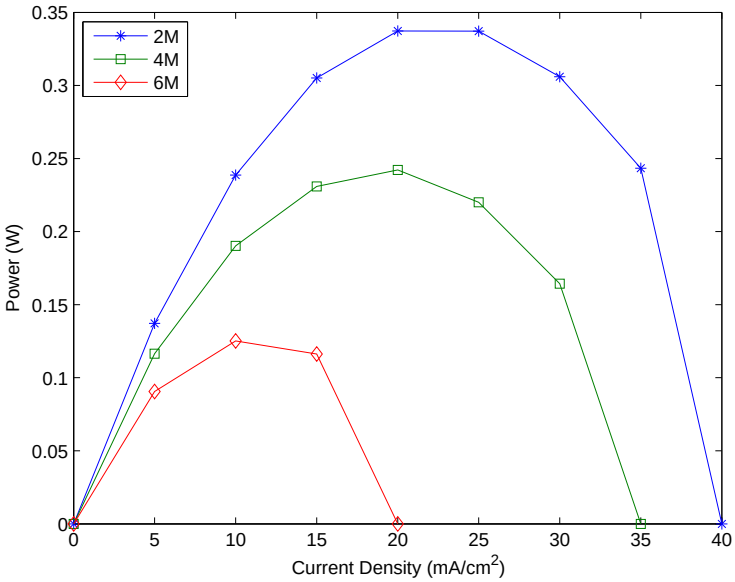


**Figure 5.6:** Power with different Concentrations — New MEA's, 60°$C$

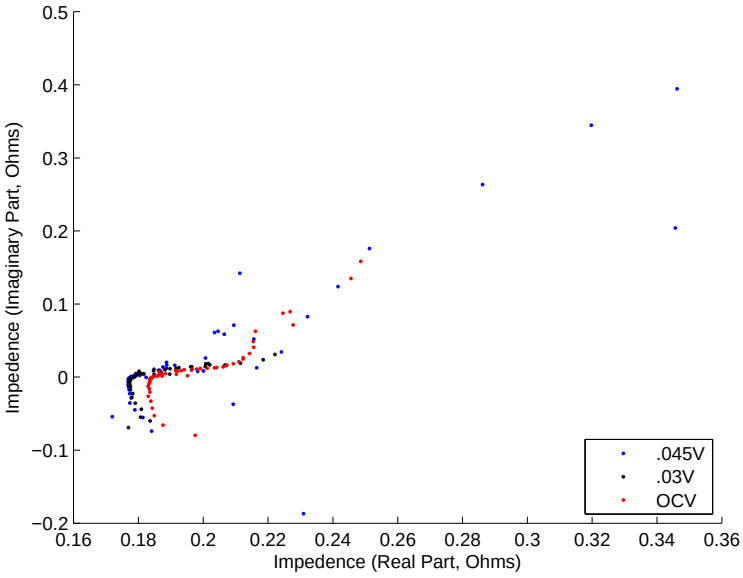


**Figure 5.7:** Impedance Spectroscopy at 4M

# Chapter 6

# DESIGN: THIRD ITERATION VERSION 2 FUEL CELL

The third iteration was changed after realizing the large amount of resistance in the cell from the electrochemical impedance spectrometry (see figure 5.7 ). A key culprit to the resistance was determined to be the lower porosity of the metal foam. In order to reduce the effect, very thin sheets of dense nickel foam (90ppi) was added as a buffer between the MEA and the aluminum foams. The effect was profound — the ohmic resistance was reduced by a factor of almost 2, from .18Ω to .10Ω (see figures 6.5, 6.6, and 6.7)

## 6.1 Standard Testing

A couple important changes were tracked in this iteration of the fuel cell design, figures 6.1 and 6.3 show the effect of fan speed on performance with the stack running on a 4M fuel, and figures 6.2 and 6.4 show the effect of fan speed on performance with the stack running on a 6M fuel. In both cases there is an impressive increase in performance by turning the fans on, and a slight increase in performance by speeding them up.

The data suggests that running the fuel cell stack with a 4M solution gives better performance than the 6M solution (due to crossover), also with the 4M solution, at higher current densities increasing the fan speed *reduces* the performance. The power curve shows similar results; with the 4M, 5V fan speed cell outputting approximately a 0.25 watts.

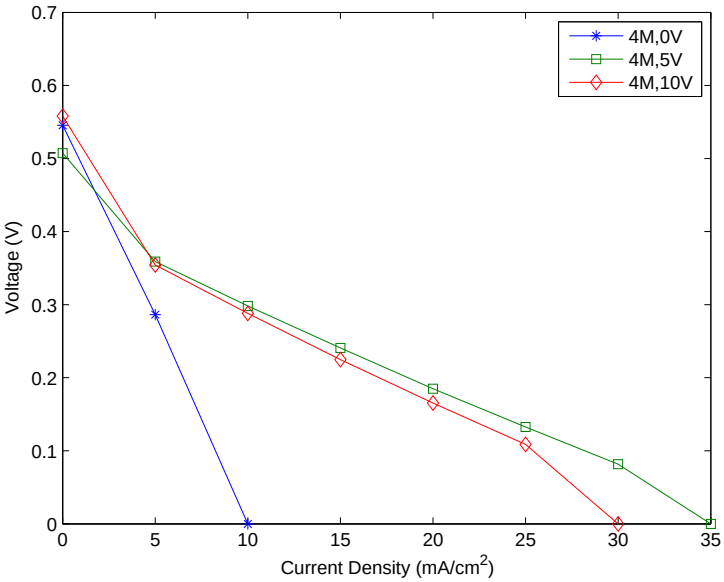


**Figure 6.1:** Polarization Curve, Passive 4M at 60°$C$, Varying Air Speed

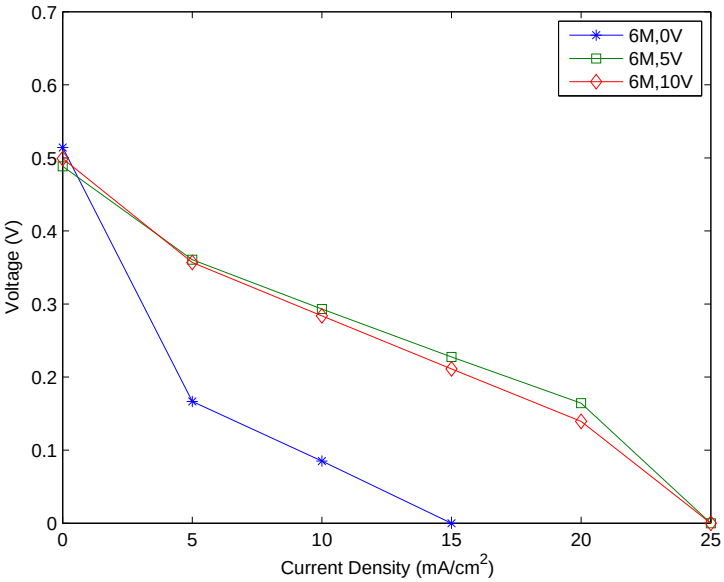


**Figure 6.2:** Polarization Curve, Passive 6M at 60°$C$, Varying Air Speed

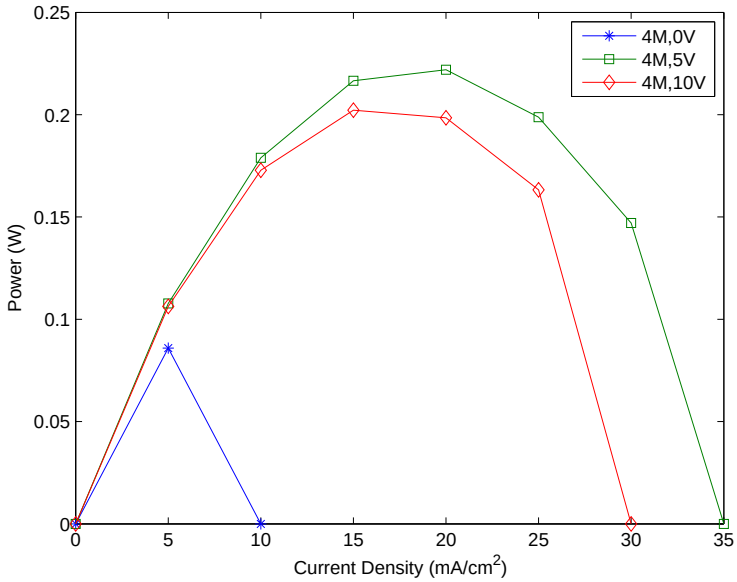


**Figure 6.3:** Power Curve, Passive 4M at $60°C$, Varying Air Speed

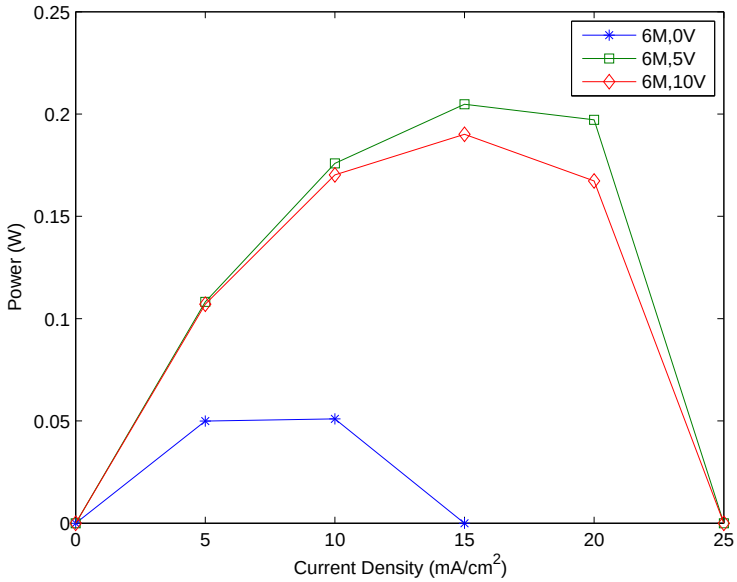


**Figure 6.4:** Power Curve, Passive 6M at $60°C$, Varying Air Speed

## 6.2 Electrochemical Impedance Spectroscopy

The main component of the electrochemical impedance spectroscopy used in this study was to observe the electrical resistance of the cell (0.1Ω in this case), however it is also possible to gain additional information from them. Most importantly, the curvature of radius of the "dome" shape in the real part vs. imaginary part plot is proportional to the amount of mass transport losses. Naturally these are insignificant at OCV, as suggested by figure 6.5, however figure 6.5 demonstrates the large effect the addition of the nickel foams in the impedance of the stack.

As voltage is decreased from OCV (figure 6.6), mass transport losses become more significant, however the lack of change by adding the fans suggests only a small amount of mass transport limitation at this voltage.

When voltage is decreased even further (figure 6.7), mass transport losses play a very significant role. The addition of the fans has a profound affect on the shape of the curve and produces a significantly large reduction in the impedance vector.

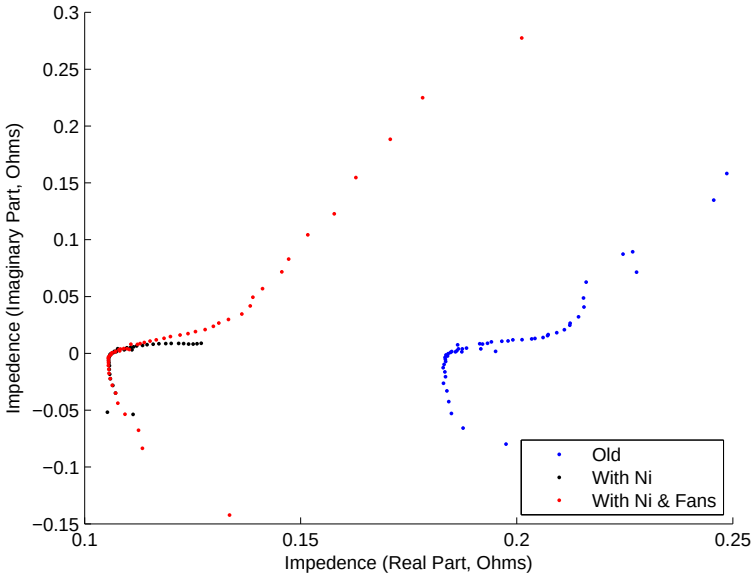


**Figure 6.5:** OCV — Impedence Spectroscopy

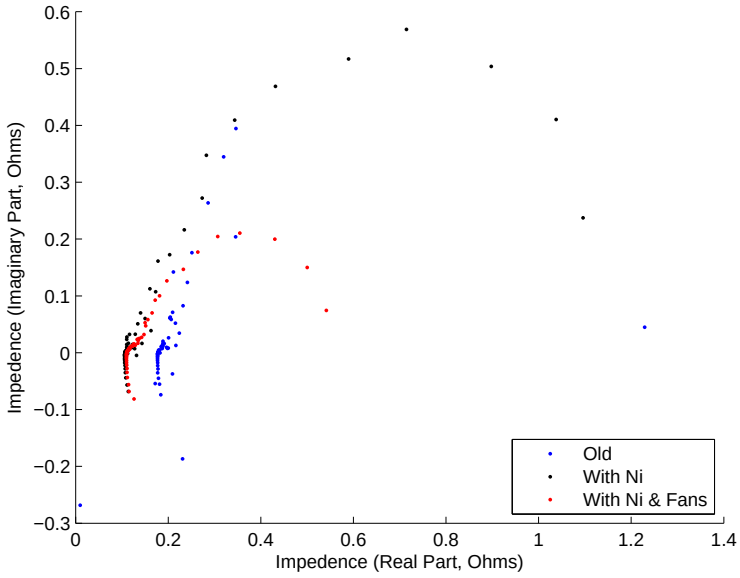


**Figure 6.6:** 0.45V — Impedence Spectroscopy

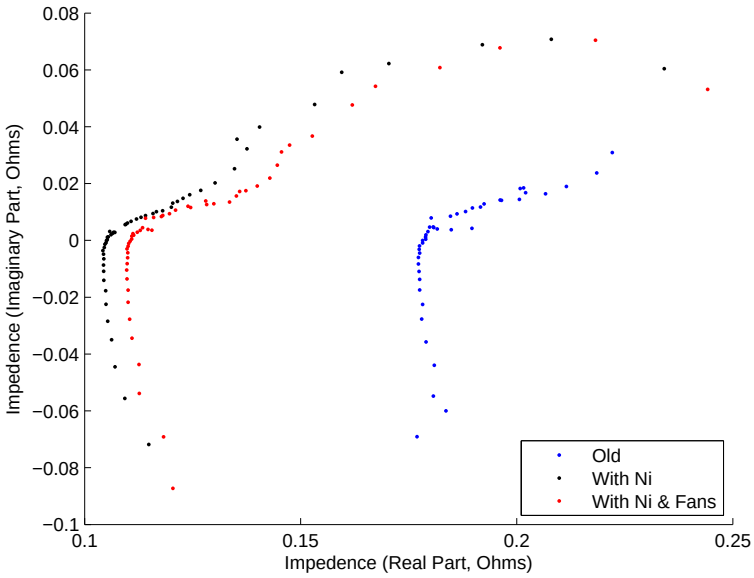


**Figure 6.7:** 0.3V — Impedence Spectroscopy

# Chapter 7

# TRANSPARENT CELL

The last and final design iteration was constructed using only one cell — this way one of the sides could be transparent, allowing for data on $CO_2$ production within the cell. Standard tests were performed, as well well as image analysis at various current densities. The tests were done with a 2M solution with and without active air. Figures 7.1 and 7.2 show the standard polarization and power curves respectively.

The data show that the new MEA improves the performance greatly, producing over 0.35 W with only one cell. The data also suggests that using active air *decreases* performance — this is due to the fact that 2M methanol was used. Because of the low concentration of the methanol, the mass transport limitations were on the anode side rather than the cathode side.

The main point of these experiments however is to determine, qualitatively, the effectiveness of the metal foam in relieving $CO_2$ bubbles from the cell. This was done by using a camera fixed to take pictures of the cell at respective current densities. Images were taken from OCV to 3000 mA in increments of 300 mA. The results provided figure 7.3 are organized from OCV (upper left) to 3000 mA (lower bottom.)

It can be seen from these results that there are no serious issues with the way the cell handles $CO_2$ transport — the bubbles disappear efficiently and do not build up to become anything serious. The implications are that a denser porosity could be used, as well as thinner foam.

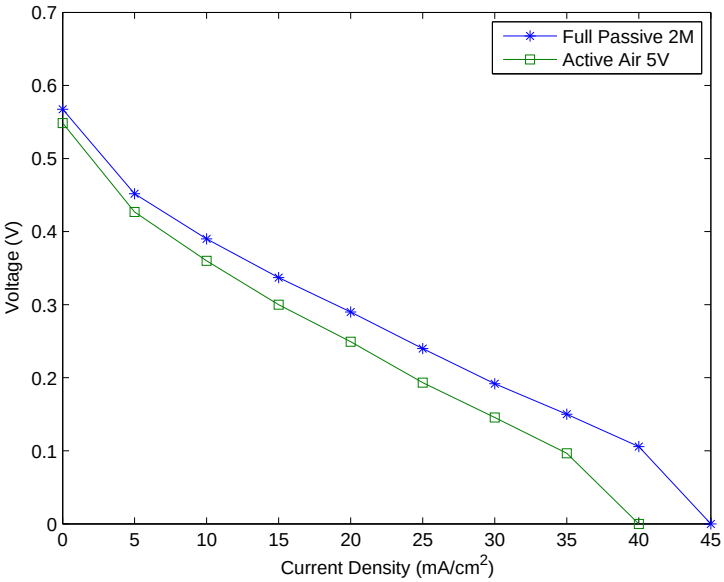


**Figure 7.1:** Polarization Curve

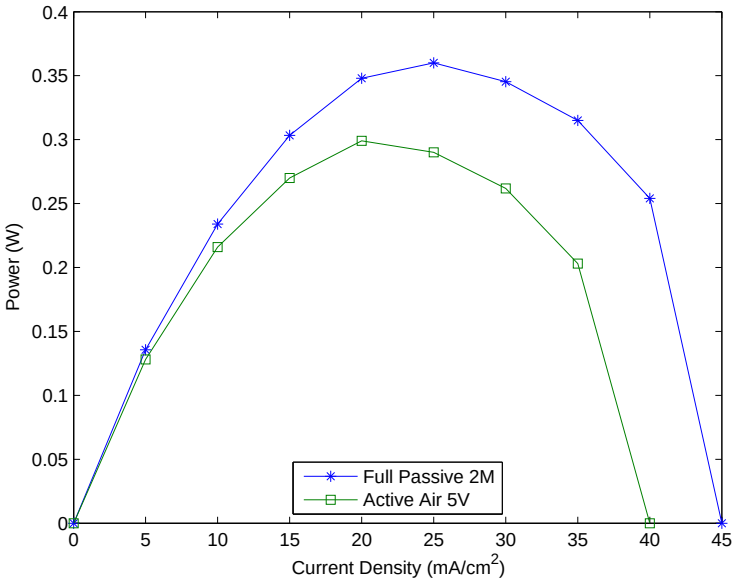


**Figure 7.2:** Power Curve

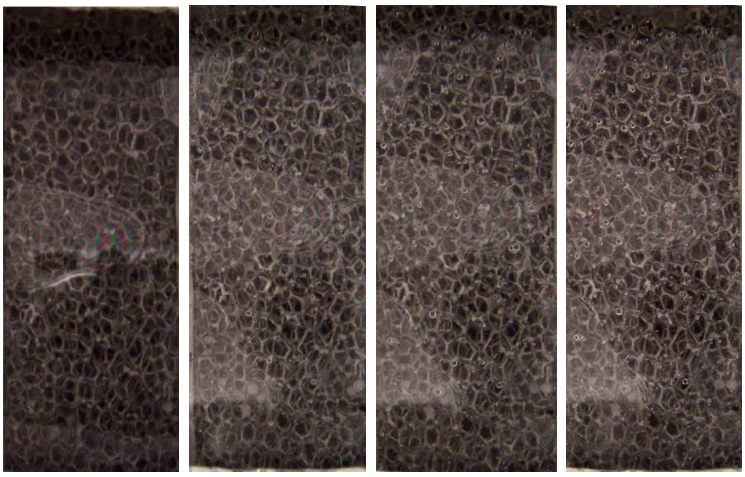

OCV — — 300mA — — 600mA — — 900mA

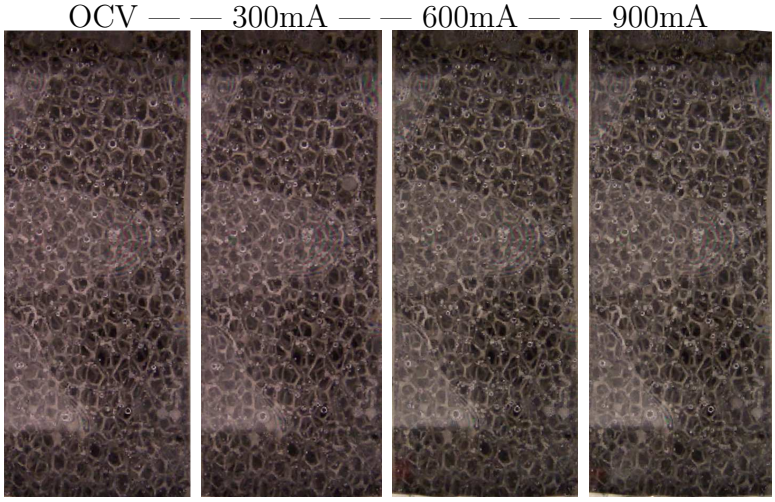

1200mA — — 1500mA — — 1800mA — — 2100mA

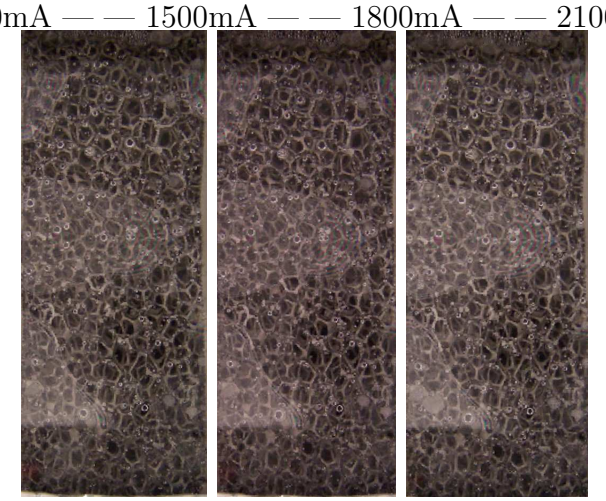

2400mA — — 2700mA — — 3000mA

**Figure 7.3:** Images

# Chapter 8

# CONCLUSIONS AND FUTURE WORK

In the future, these results need to be applied to a larger stack that can be used for a practical purpose. The work done shows that there are a lot of challenges that are added when a fuel cell stack is purposed for a practical application rather than a laboratory bench.

The largest addition required for a practical stack will be a more advanced balance of plant. The practical stack will need several features. It will need to be able to regulate its output power to remain optimal, as well as initiate and control a startup sequence.

The largest problems that can be foreseen in a practical stack are thermal management and ohmic losses. Both of these problems can be helped by making the stack smaller. Thermal management is only a problem at boot up — the cell will have a quicker startup if heaters are embedded in it to aid in increasing the temperature. Depending on the size of the stack (active area) it may need to be insulated. Ohmic losses can be reduced by decreasing the pore size of the metal foam and by making it thinner.

However, there is a problem that arises when making the stack smaller — both on the anode and cathode sides. As the cell gets smaller its current fuel capacity will be reduced and it's ability to remove $CO_2$ will be reduced. The fuel capacity issue can be reduced by using a manifold and storage system, a proposed system would use Pascal's law to maintain perfect level of the fuel on the anode

side. Experiments can be performed with relative ease to identify the practicality of this design (see chapter7).

Another very important feature that is necessary in a stack is cell voltage monitoring. As seen in section 5.2.5 it is possible for one unhealthy cell to bring down the whole stack; it is also very impractical to need to re-wire the stack before being able to independently measure voltages and currents.

In conclusion there are many hurdles left to overcome before a real practical stack can be manufactured and tested which has a reasonable size and performance, however, current technology is well on it's way to realizing this and with a bit more research it seems that the next generation of portable power will be able to run off of methanol.

# REFERENCES

Srikanth Arisetty, B.S.; Cedric A Jacob; Ajay K Prasad, Ph.D.; Suresh Advani "Regulating methanol feed concentration in direct methanol fuel cells using feedback from voltage measurements," Journal of Power Sciences, 2008

James Larminie; Andrew Dicks "Fuel Cell Systems Explained," John Wiley & Sons Ltd, 2003